Supporting Information

Niedbala et al. 10.1073/pnas.1100667108

SI Materials and Methods

Mice. BALB/c mice were obtained from Harlan Olac, and *Nos2*$^{-/-}$ (B6.129P2-Nos2$^{tm/Lau}$) mice and WT B6 mice were obtained from the Jackson Laboratory. *Ahr*$^{-/-}$, *Il2*$^{-/-}$, and *Il10*$^{-/-}$ mice of the B6 background were obtained from the National Institute of Medical Research, Mill Hill, London, United Kingdom. *Il1r1*$^{-/-}$ (1) mice of the B6 background were obtained from the Centre National de la Recherche Scientifique, Orleans, France. All animal experiments were performed according to institutional guidelines and national regulations.

Murine Cell Culture. To polarize Th17 cells, CD4$^+$ T cells were purified from the pool of spleens and lymph nodes of naive mice by means of an AutoMacs (Miltenyi Bioscience) using negative selection (routine purity >98%). Culture medium was RPMI-1640 supplemented with 10% (vol/vol) FCS (LONZA), 2 mM L-glutamine, 100 U/mL penicillin, 100 μg/mL streptomycin, and 0.05 M 2-mercaptoethanol. The cells were cultured (6×10^5 cells/mL) for up to 5 d in round-bottom 96-well plates (Costar) with mitomycin-C–treated spleen cells (antigen-presenting cells), soluble anti-CD3 antibody (1 μg/mL; BD Bioscience), and a mixture of cytokines (TGF-β, 1 ng/mL; IL-6, 10 ng/mL; and IL-1β, 10 ng/mL; all from R&D Systems) in the presence or absence of a combination of antibodies (anti–IL-4, anti–IFN-γ, and anti–IL-2; all from R&D Systems) and used at 10 μg/mL as described previously (2). *Ahr*$^{-/-}$ cells were cultured in flat-bottom 96-well plates with plate-bound anti-CD3, anti-CD28, and the same mixture of cytokines and antibodies as above. To polarize Th1 and Th2 cells, different culture conditions were used according to published optimized protocols: for Th1, 10 ng/mL IL-12 and 10 μg/mL anti–IL-4 (both from R&D Systems), and for Th2, 10 ng/mL IL-4 and 10 μg/mL anti–IFN-γ and anti–IL-12 (all from R&D Systems). At the end of cultures, supernatants were collected for cytokine assay by ELISA and the cells were stained for intracellular cytokine and transcription factors by FACSCalibur (BD Bioscience). Some cells were extracted for mRNA for qPCR analysis. In some cultures, graded concentrations of NOC-18 {(Z)-1-[2-(2-Aminoethyl)-*N*-(2-ammononioethyl) amino]diazen-1-ium-1,2-diolate}, also known as DETA-NONOate (Alexis), were added at the beginning of the culture. In some experiments, the AHR ligand FICZ (BioMol) was also added at the start of the culture. Blast formation was determined by FACS forward scattering and propidium iodide staining, and apoptosis/necrosis was determined using the annexin V and propidium iodide kit (PharMingen). Cell division was determined by labeling with CFSE (Molecular Probes, Inc.), and florescence density was analyzed by FACS. For measurement of intracellular cytokines, T cells were restimulated with 50 ng/mL phorbol-12-myristate-13-acetate and 500 ng/mL ionomycin (both from Sigma) in the presence of GolgiStop (BD Bioscience) for 4 h. The cells were first stained for CD4, then permeabilized with Perm/Fix solution (eBioscience), and finally stained with anti–IL-17A, anti-RORγt, anti–IL-22 or anti-foxp3 (all from eBioscience), anti-IL-4, anti-IL-10, anti-IFNγ, pSTAT-3 (BD Bioscience) or IRF4 (Santa Cruz Biotechnology) and analyzed by FACS. For receptor expression, cells were stained with anti–IL-1R1 (BD Bioscience), anti-gp130 (R&D Systems), or anti–TGF-βRII (R&D Systems). Isotype-matched rat antimouse antibodies (directly conjugated) were used as controls.

Human Cell Culture. Peripheral blood was obtained from healthy volunteers after obtaining informed consent. Mononuclear cells were purified by Ficoll–Paque Plus (GE Healthcare), followed by CD4$^+$ T-cell isolation using AutoMac. The cells were cultured (1×10^6/mL) for 4 d in round-bottom 96-well plates (Costar) with Dynabead (4×10^7/mL; Invitrogen)-coated anti-hCD3, anti-hCD28, hIL-6 (25 ng/mL; R&D Systems), hTGF-β (2.5 ng/mL; eBioscience), hIL-1β (10 ng/mL; R&D Systems), hIL-21 (10 ng/mL; eBioscience), hIL-23 (10 ng/mL; eBioscience) and anti–hIFN-γ and anti–hIL-4 (both 10 μg/mL; R&D Systems) antibodies in the presence of graded concentrations of NOC-18. At the end of culture, supernatants were harvested for ELISA of IL-17A and IL-10, and the cells were stained for intracellular IL-17A and IL-22 (R&D Systems) and analyzed by FACS. The cells were also stained for propidium iodide and Annexin V to assay for necrosis and apoptosis as described above.

RNA Isolation and qPCR. mRNA in CD4$^+$ T cells was isolated 24–72 h after Th17 differentiation using the RNeasy Mini kit (Qiagen). Spinal cord mRNA from WT and *Nos2*$^{-/-}$ mice was isolated on day 17 after immunization using the TRIzol extraction method (Gibco). RT was performed with 500 ng of total RNA using the Applied Biosystems cDNA kit. qPCR was performed with the Sybr Green or TaqMan Gene Expression Assay using the ABI Prism 7900 Sequence Detection System instrument (Applied Biosystems) according to the manufacturer's protocol. Expression was normalized to the housekeeping gene *Hprt*. The sequences for primers and probes are as follows: *Il17a*: forward, 5′-CTC CAG AAG GCC CTC AGA CTA C-3′ and reverse, 5′-GGG TCT TCA TTG CGG TGG-3′; *Il17f*: forward, 5′-TGC TAC TGT TGA TGT TGG GAC-3′ and reverse, 5′-AAT GCC CTG GTT TTG GTT GAA-3′; *Il21*: forward, 5′-TCA TCA TTG ACC TCG TGG CCC-3′ and reverse, 5′-ATC GTA CTT CTC CAC TTG CAA TCC C-3′; *Il22*: forward, 5′-CAT GCA GGA GGT GGT ACC TT-3′ and reverse, 5′-CAG ACG CAA GCA TTT CTC AG-3′; *Ahr*: forward, 5′-CAA ATC AGA GAC TGG CAG GA-3′ and reverse, 5′-AGA AGA CCA AGG CAT CTG CT-3′; *Rora*: forward, 5′-TCT CCC TGC GCT CTC CGC AC-3′ and reverse, 5′-TCC ACA GAT CTT GCA TGG A-3′; *Ets1*: forward, 5′-CCG ACT CTC ACC ATC ATC AA-3′ and reverse, 5′-GAA CTC ATT CAC AGC CCA CA-3′; *Cyp1a1*: forward, 5′-CCT CTT TGG AGC TGG GTT T-3′ and reverse, 5′-AGG CTC CAC GAG ATA GCA GT-3′; *Nos2*: forward, 5′-CGA AAC GCT TCA CTT CCA A-3′ and reverse, 5′-TGA GCC TAT ATT GCT GTG GCT-3′; *Hprt*: forward, 5′-GCA GTA CAG CCC CAA AAT GG-3′, reverse, 5′-AAC AAA GTC TGG CCT GTA TCC AA-3′, and probe, 5′-TAA GTT GCA AGC TTG CTG GTG AAA AGG A-3′; *Rorc*: forward, 5′-CCG CTG AGA GGG CTT CAC-3′, reverse, 5′-TGC AGG AGT AGG CCA CAT TAC A-3′, and probe, 5′-AAG GGC TTC TTC CGC CGC AGC CAG-3′; *Il23r*: primers from Applied Biosystems (Mm00519937_A1).

Western Blotting. AHR protein levels were analyzed in CD4$^+$ T cells under the Th17 polarization condition in the presence or absence of NOC-18 on day 3. Proteins were detected using antibodies against AHR (BioMol) or β-actin (Abcam), followed by HRP-conjugated goat anti-rabbit antibody (Pierce) and an ECL kit (GE Healthcare). The relative intensities of the bands were quantified using Image J software (National Institutes of Health), and all the values were normalized to the intensities of the respective β-Actin signal.

EAE Induction. EAE was induced by injecting mice s.c. with 100 μg of the $MOG_{35–55}$ peptide in complete Freund's adjuvant containing 200 μg of *Mycobacterium tuberculosis* H37Ra (Difco Laboratories). Pertussis toxin (Sigma–Aldrich) was injected (300 ng, i.p.) at the time of immunization and 48 h later. Clinical signs of EAE were assessed daily according to the following scores based on a 10-point scale: 0, no detectable signs; 1, distal section of tail paralyzed; 2, distal and proximal sections of tail paralyzed; 3, distal and proximal sections of tail paralyzed and hind-limb weakness; 4, unilateral partial hind-limb paralysis; 5, bilateral partial hind-limb paralysis; 6, complete bilateral hind-limb paralysis; 7, complete hind-limb paralysis and forelimb weakness; 8, complete hind-limb paralysis and unilateral forelimb paralysis; 9, complete hind-limb paralysis and total paralysis of forelimb; and 10, death. Because endpoints were restricted in the animal experimentation guidelines in some animal facilities, in some experiments, the disease was also scored according to a 5-point scale: 0, no clinical signs; 1, complete loss of tail tone; 2, hind-limb weakness; 3, hind-limb paralysis; 4, forelimb involvement; and 5, moribund. Serum and spinal cord samples were collected 17 d after EAE induction for analysis. Draining lymph node cells were isolated on day 17 after immunization and stimulated in culture medium containing 50 $\mu g \cdot mL^{-1}$ $MOG_{35–55}$ or 5 $\mu g \cdot mL^{-1}$ ConA (Sigma) for 96 h. Supernatants were harvested, and IL-17A and IFN-γ concentrations were determined by ELISA. In addition, an IL-17 neutralization experiment was performed with a monoclonal anti–IL-17 antibody (MAB421; R&D Systems), and IgG2A isotype (MAB006; R&D Systems) was used as a control. Mice were injected i.p. with 100 μg of neutralizing antibody or isotype control at days 6, 8, 10, 12, and 14 after immunization. Clinical signs of EAE were assessed daily according to the following scores based on a 5-point scale. The treatment experiments were graded by a blinded observer.

Immunofluorescence. Cryostat sections (5 μM) of spinal cords were fixed in acetone, dried, and rehydrated. Sections were incubated with 3 μg/mL rabbit anti-CD3 polyclonal antibody (DAKO). For detection, an isotype-specific secondary Alexa Fluor 594-conjugated antibody was used (Invitrogen). Sections were then incubated with 2 μg/mL goat anti-mouse IL-17A (R&D Systems), followed by incubation with anti-goat IgG-HRP conjugate (1:100). For detection, an AF488-labeled tyramide amplification kit (Invitrogen) was used. Tyramide signal amplification is an enzyme-mediated detection method that uses the catalytic activity of HRP to generate high-density labeling of a target protein. A negative staining control was performed by incubation with isotype control antibody for the first incubation. Fluorescence images were taken using a fluorescence microscope connected to a Hamamatsu Orca ER digital camera and the Openlab version 3.0.9 digital imaging program (Improvision). The sections were also stained with H&E and examined under low power to investigated total cellular infiltration.

ELISA. ELISAs were carried out with paired antibodies according to the manufacturer's instructions: mouse IL-17A, IL-17F, IL-2, IL-10, IL-4, IFN-γ, and human IL-17A and IL-10 (all from BD Bioscience). The sensitivity of the assays was <50 pg/mL.

Statistical Analysis. Clinical and histological scores were analyzed with the nonparametric Mann–Whitney *U* test. Differences between cumulative incidences at a given time point were analyzed by χ^2 contingency analysis. Cellular proliferation and cytokine levels were compared using the Student *t* test. All experiments were performed at least two times ($^*P < 0.05$; $^{**}P < 0.01$).

1. Labow M, et al. (1997) Absence of IL-1 signaling and reduced inflammatory response in IL-1 type I receptor-deficient mice. *J Immunol* 159:2452–2461.

2. Niedbala W, et al. (2007) IL-35 is a novel cytokine with therapeutic effects against collagen-induced arthritis through the expansion of regulatory T cells and suppression of Th17 cells. *Eur J Immunol* 37:3021–3029.

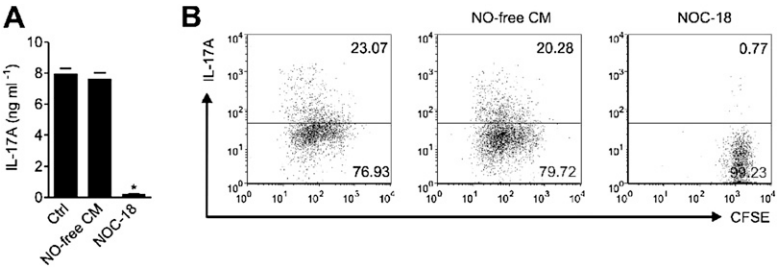

Fig. S1. NO suppresses Th17 cells independent of NO-induced metabolites. $CD4^+$ T cells from BALB/c mice were polarized to Th17 cells with freshly added NOC-18 (200 μM) or NO-free culture medium, which was medium with 200 μM NO-18 added 5 d previously. Cells were also labeled with CFSE. (*A*) The cultures were terminated on day 4, and the concentrations of IL-17A in culture supernatant were determined by ELISA. (*B*) Cells were also analyzed for $IL\text{-}17A^+$ cells and cell cycle (CFSE dilution) by FACS. Freshly added NOC-18 effectively suppressed Th17 differentiation, whereas the NO-free condition medium did not. Data are representative of two independent experiments. Ctrl, control.

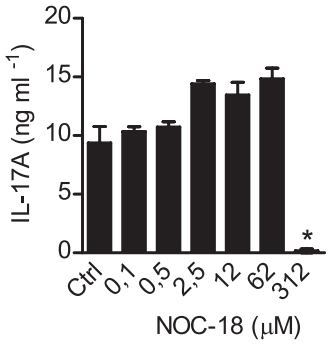

Fig. S2. NOC-18 at low concentrations had no effect on Th17 polarization. $CD4^+$ T cells from BALB/c mice were polarized to Th17 for 5 d in the presence of fivefold dilutions of NOC-18. IL-17A concentrations in the supernatants were determined by ELISA. Data are mean ± SEM (n = 3), representative of two experiments. *$P < 0.05$. Ctrl, control.

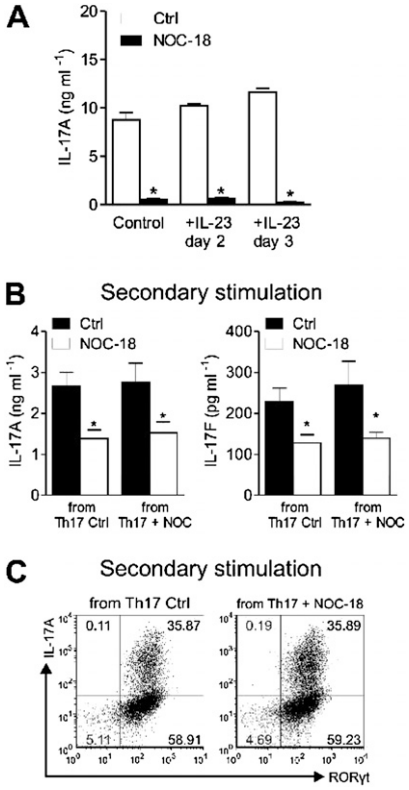

Fig. S3. Continuous presence of NO is required to suppress Th17 activity. (*A*) Th17 cells are not responsive to IL-23 in the presence of NO. $CD4^+$ T cells from BALB/c mice were polarized to Th17 in the presence of 200 μM NOC-18, and IL-23 (20 ng/mL) was added on day 2 or 3 of culture. Culture supernatants were harvested on day 5, and IL-17 concentrations were determined by ELISA. Data are mean ± SEM (n = 4), representative of two experiments. *$P < 0.05$. Ctrl, control. (*B*) $CD4^+$ T cells were polarized to Th17 ± 200 μM NOC-18 for 5 d. The cells were washed and restimulated with anti-CD3 and IL-23 (20 ng/mL) ± 200 μM NOC-18 for 3 d. IL-17A concentration in the culture supernatant was determined by ELISA. Data are mean ± SEM (n = 4), representative of two experiments. *$P < 0.05$. (*C*) Cells were cultured as in *B* without adding NOC-18 a second time. Intracellular staining of IL-17A was performed by FACS on day 3. Data are representative of three experiments.

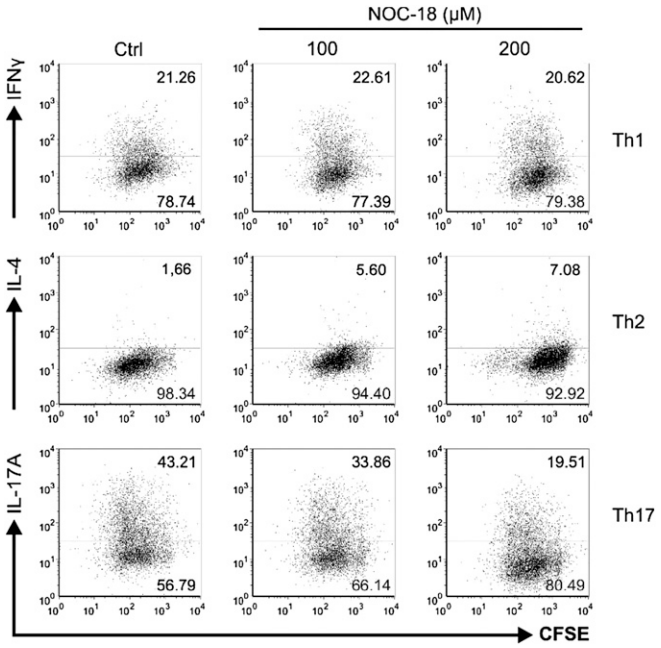

Fig. S4. At high concentrations, NO suppressed Th17 polarization and enhanced Th2 differentiation but had no effect on Th1 development. CD4$^+$ T cells from BALB/c mice were polarized to Th17, Th1, and Th2 cells under the conditions (*SI Materials and Methods*) for 3 d in the presence or absence of NOC-18 as indicated. Intracellular staining for IFN-γ, IL-4, and IL-17A was performed by FACS. Data are representative of three experiments. Ctrl, control.

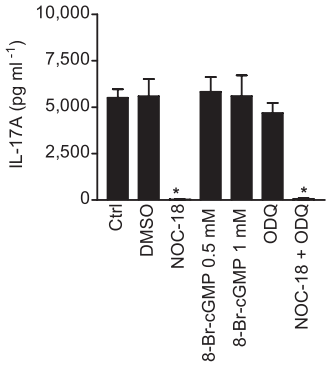

Fig. S5. NO suppresses Th17 development independent of cGMP. Purified CD4$^+$ T cells from BALB/c mice were cultured for 3 d under the Th17 polarizing condition in the presence of medium alone or with DMSO (diluent), NOC-18 (200 μM), 8-Br–cGMP (0.5–1 mM, an analog of cGMP), or ODQ (10 μM, a competitive inhibitor of the activation of cGMP). The concentrations of 8-Br–cGMP and ODQ used could effectively activate or inhibit sGC, respectively. IL-17A concentration in the culture supernatant was determined by ELISA. NO effectively suppressed IL-17A synthesis, whereas 8-Br–cGMP did not. ODQ did not reverse the NO-mediated suppression of IL-17A synthesis. $n = 5$. *$P < 0.001$. Similar results were obtained with established Th17 cells. Ctrl, control.

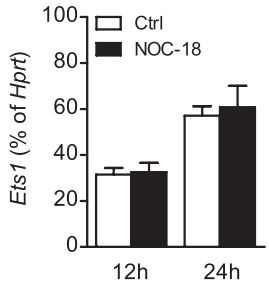

Fig. S6. NO does not affect the expression of *Ets1*. Purified CD4$^+$ T cells from BALB/c mice were cultured under the Th17 polarizing condition with or without NOC-18 (200 μM). Cells were harvested at 12 or 24 h, and mRNA expression was determined by qPCR. Data are representative of two independent experiments. Ctrl, control.

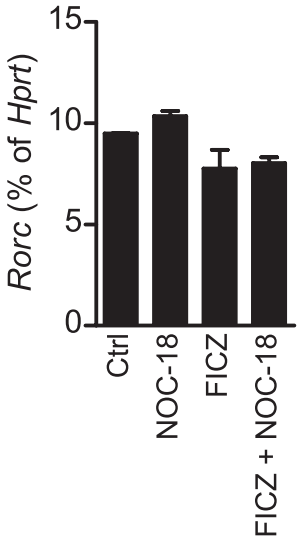

Fig. S7. FICZ and NO do not affect *Rorc* expression. CD4$^+$ T cells from BALB/c mice were polarized to Th17 in the presence or absence of FICZ (200 nM) and NOC-18 (200 μM) for 3 d, and the cells were harvested and assayed for the expression of *Rorc* mRNA by qPCR. Data are representative of two independent experiments. Ctrl, control.

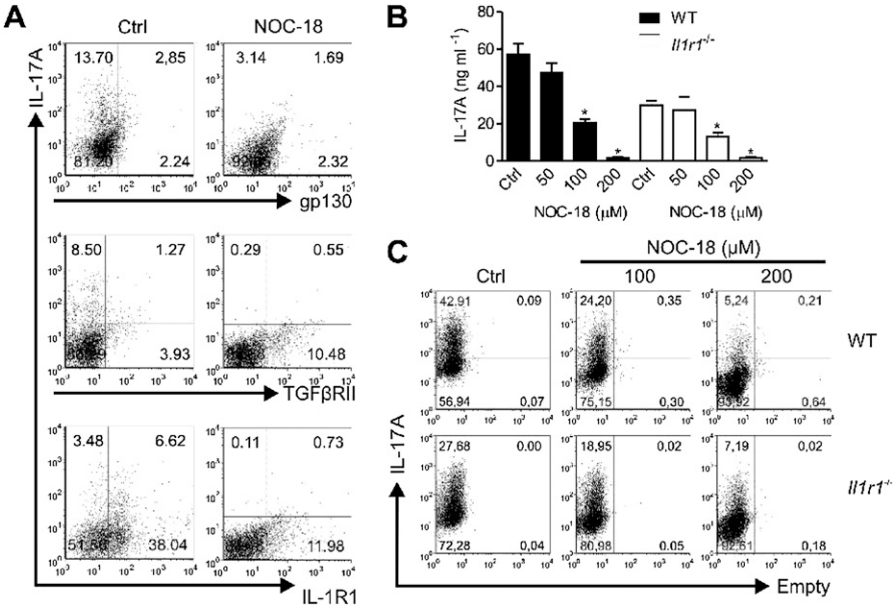

Fig. S8. NO suppresses IL-1R1 expression, but NO can further suppress Th17 differentiation in *Il1r1*$^{-/-}$ cells. (*A*) CD4$^+$ T cells from B6 mice were polarized to Th17 ± 200 μM NOC-18 for 2 d. The expression of IL-1R1, IL-6R (gp130), and TGF-βRII was determined by FACS. Data are representative of three experiments. Ctrl, control. (*B*) CD4$^+$ T cells from WT B6 mice or B6 *Il1r1*$^{-/-}$ mice were polarized to Th17 for 5 d in the presence of graded concentrations of NOC-18. IL-17A concentrations in the culture supernatant were determined by ELISA. Data are mean ± SEM ($n = 4$), representative of two experiments. *$P < 0.05$. (*C*) Cells were polarized as in *B* above, and intracellular IL-17A was stained and analyzed by FACS. Data are representative of three experiments.

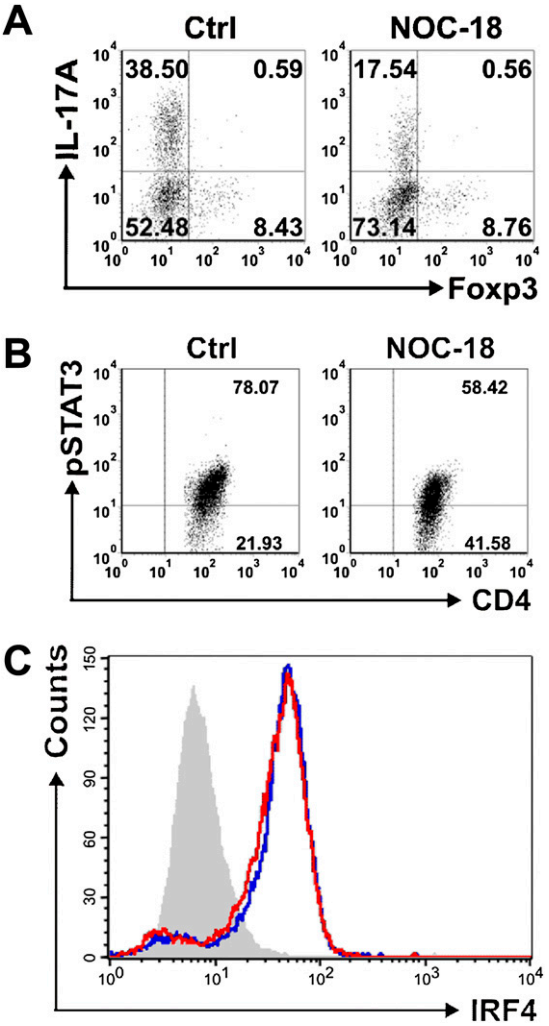

Fig. S9. NO does not affect Foxp3 and IRF4 expression but suppresses Stat3 phosphorylation. $CD4^+$ T cells from BALB/c mice were polarized to Th17 with or without NOC-18 (200 μM) for 4 d and stained intracellularly for IL-17A vs. Foxp3 (*A*) or p-Stat3 vs. CD4 (*B*). Ctrl, control. (*C*) $CD4^+$ T cells from B6 mice were polarized to Th17 with or without NOC-18 (100 μM) for 4 d and stained for IRF4. The histogram shows isotype control (gray), Th17 without NOC-18 (blue), and Th17 with NOC-18 (red). The NO treatment reduced Th17 polarization from 42 to 14%. Data are representative of two experiments.

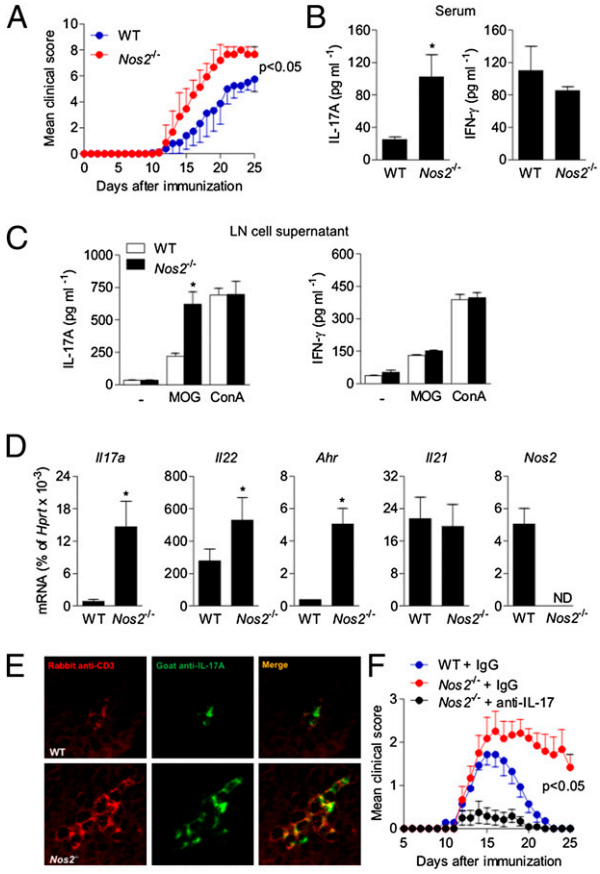

Fig. S10. *Nos2*$^{-/-}$ mice developed exacerbated EAE, elevated numbers of Th17 cells, and enhanced AHR expression. (*A*) WT or *Nos2*$^{-/-}$ mice were induced for EAE, and disease development was scored. Data are mean ± SD (n = 20 mice per group) pooled from four experiments. The score was based on a 10-point scale. (*B*) Serum was obtained on day 17 and IL-17A and IFN-γ concentrations determined by ELISA. *$P < 0.05$ from day 20–25. (*C*) Draining lymph nodes were harvested on day 17 and cultured with $MOG_{35–55}$ antigen or ConA for 4 d, and cytokines in the culture supernatant were determined by ELISA. (*D*) Expression of *Il17a*, *Il21*, *Il22*, *Ahr*, and *Nos2* mRNA in the spinal cord on day 17 was determined by qPCR. (*E*) Representative immunofluorescence images of spinal cord sections stained for CD3$^+$ IL-17$^+$ T cells in the *Nos2*$^{-/-}$ and WT mice are shown. Larger magnification is shown in Fig. S11. (*F*) WT or *Nos2*$^{-/-}$ mice were induced for EAE, and the effect of IL-17 neutralization was determined in *Nos2*$^{-/-}$ mice. Mice were injected i.p. with 100 μg neutralizing anti–IL-17 antibody or isotype control after immunization. The clinical score was based on a five-point scale. (*C*–*F*) Data are mean ± SEM (n = 5), representative of two independent experiments. *$P < 0.05$ (compared with WT mice).

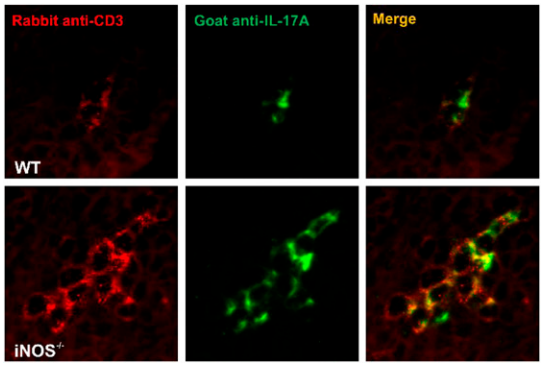

Fig. S11. Higher magnification of the immunofluorescent staining in Fig. S10*E* of CD4$^+$ IL-17$^+$ T cells in the spinal cord of WT and *Nos2*$^{-/-}$ mice with EAE.